# Rigorous modeling and experimental validation of mass, charge and energy transport in a DMFC polymer electrolyte membrane

*Thorsten Schultz[1], Kai Sundmacher[1,2]*

[1]  *Max Planck Institute Dynamics of Complex Technical Systems*
   *Sandtorstrasse 1, 39106 Magdeburg, Germany*
   *phone +49-391-6110-350, fax +49-391-6110-353*
   *sundmacher@mpi-magdeburg.mpg.de*

[2]  *Process Systems Engineering, Otto-von-Guericke University Magdeburg*
   *Universitätsplatz 2, 39106 Magdeburg , Germany*

## Introduction

In the past few years, the interest in the Direct Methanol Fuel Cell (DMFC) has increased dramatically, as it has very advantageous features as a mobile source of electrical energy. Its fuel - methanol - is easy to store and to handle and has a high energy density. These advantages over hydrogen-fed PEMFCs (polymer electrolyte membrane fuel cells) have resulted in first commercial products (e.g. from SmartFuelCell, Germany, www.smartfuelcell.de).

Nonetheless, the DMFC suffers from well known significant material problems (for a broad overview see e.g. the review papers by CARRETTE et al.  [1]  and SCHULTZ et al. [2] ). One problem is the low activity of the platinum-ruthenium anode catalysts, the other is the permeation of methanol from the anode side through the polymer electrolyte membrane (PEM) to the cathode catalyst (methanol crossover). Methanol is oxidised at the cathode with oxygen, leading to a mixed potential which results in a significantly reduced overall cell voltage, and due to the loss of methanol also to a reduced fuel efficiency. Moreover, also water crosses the PEM (water crossover), which can, combined with the water production from the cathode reactions, lead to condensation in the cathode pore structure and flowbed, blocking the way for fresh oxygen and thus resulting in a significantly reduced performance. These phenomena (and some others like e.g. carbon dioxide bubble formation on the anode side) are responsible for the DMFC reaching maximum power densities which are typically much below those reached with PEMFCs [2] [3] . Figure 1
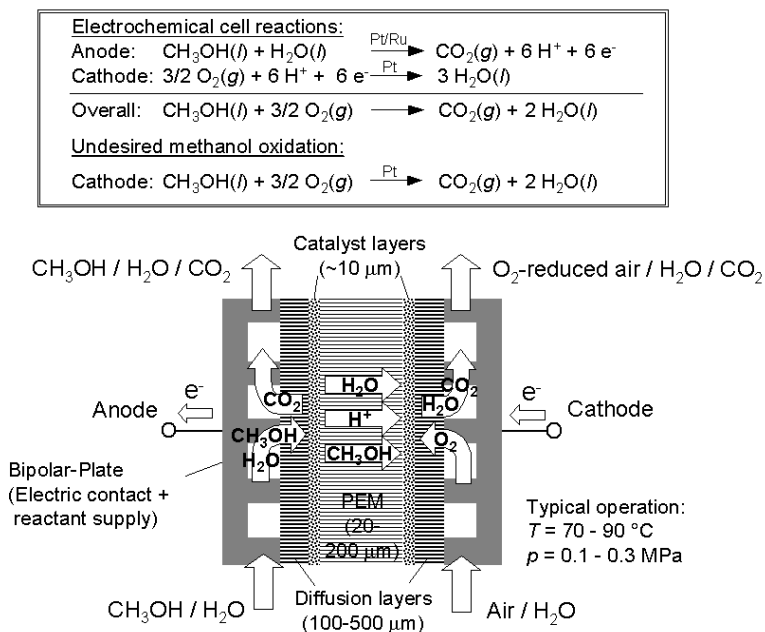


**Figure 1** Structure and principle of the DMFC [2]

presents the structure of the DMFC, the occuring electrochemical and chemical reactions and the transport paths for all important components.

As methanol and water crossover play a key role in the DMFC, these phenomena have to be accounted for correctly in mathematical process models. Unfortunately the conventional membrane materials (sulfonated fluoropolymers, like e.g. NAFION™ by DuPont) exhibit some properties, which make a realistic model description using classical mass transport models (Fick diffusion and Nernst-Planck models like e.g. used in [4] [5] [6] ) difficult. The typical PEM material shows significant swelling when in contact with water, and even more so when in contact with methanol. The swollen material is nanoporous (pore diameters in the range of 1-4 nm [2] ), with regions where only the polymer backbone material can be found, and a pore system filled with water and methanol. At the pore walls, sulfonic acid groups are attached. The pore water solvatises the protons, making them mobile within the pore system.

**Mass transport model of the PEM**

In the DMFC model, the supply channels and both catalyst layers are described as spatially concentrated volume elements (CSTR behaviour), while both diffusion layers and the PEM are modelled as spatially distributed elements along the z-coordinate perpendicular to the cell plane. The geometries of all elements are assumed to be fixed (solid matrices with given porosities and thicknesses), except for the PEM. Here swelling is accounted for, but for simplification all local volume changes are only attributed to changes in thickness along the z-coordinate.

For the description of mass transport the generalised Maxwell-Stefan approach for mass transport in porous structures is used, as suggested by KRISHNA and WESSELINGH [7] [8] . It is based on a mechanical equilibrium between driving forces acting on a species $j$ and the friction between this species and all other species $i$ around it:

$$-\frac{c_j}{RT}\nabla_{T,p}\mu_j - \frac{c_j}{RT}\overline{V}_j \nabla p - \frac{\alpha_j{}'}{\DJ_{jM}}c_j\frac{B_0}{\eta^{vis}}\nabla p - c_j z_j^* \frac{F}{RT}\nabla\phi$$
$$=\sum_{i\neq j}\frac{x_i n_j - x_j n_i}{\DJ_{ij}^{eff}} + \frac{n_j}{\DJ_{jM}^{eff}}$$

(1)

On the left hand side of equation (1) four terms are summing up the driving forces. The first and second term represent forces due to gradients in the chemical potentials $\mu_j$ [J mol$^{-1}$] (first term: at constant pressure, second term: pressure influence), i.e. resulting in diffusive fluxes. The third term is a driving force due to a gradient in the total pressure $p$ [Pa] (i.e. viscous flow). The fourth term represents driving forces due to a gradient of the electric potential field $\phi$ [V] (i.e. electro-migration). On the right hand side are two terms describing friction: The first accounts for the friction forces between species $j$ and all other mobile species $i$ ( $x_j$ [-] are mole fractions, $n_j$ [mol m$^{-2}$ s$^{-1}$] are flux densities), and the second term represents friction forces between species $j$ and the (stationary) solid matrix (index "$M$") of the PEM. The most important parameters in this equation are the binary Maxwell-Stefan diffusion coefficients $\DJ$ [m$^2$ s$^{-1}$]. The lower indices denote the two respective species, the upper index "$eff$" indicates an effective diffusion coefficient taking into account the porosity and the tortuosity of the solid matrix. Other symbols in equation (1) are the molar concentrations $c_j$ [mol m$^{-3}$], the hydraulic permeability $B_0$ [m²], the universal gas constant $R$ =8.314 J mol$^{-1}$ K$^{-1}$, the local temperature $T$ [K], Faraday´s

constant $F = 96485$ C mol$^{-1}$, the molar volume $\overline{V}_j$ [m³ mol-1], the viscous selectivity coefficient $\alpha_j'$ [-], the dynamic viscosity $\eta^{vis}$ [Pa s] and the charge number $z_j^*$ [-] of species $j$.

In many mass transport processes, the chemical potential gradients can be approximated by the gradients in the mole fractions as the species activity coefficients are nearly constant. This then simplifies the first term of equation (1), and such approaches have already been used for transport models in PEMFCs (see e.g. [9] ). However, such an approach can not be applied for the DMFC, as here on one side (anode) liquid water as excess component is present, while on the other side (cathode) water is only present as usually minor component in air. Therefore in the DMFC on both sides of the PEM one can expect to find totally different water contents in the PEM material, and therefore totally different degrees of swelling and a pronounced water concentration (and therefore also activity) profile have to be expected. The same is true for methanol, which is present on the anode side in significant amounts, while on the cathode it can be assumed to be immediately consumed, so that the cathode side of the PEM contains only negligible amounts of methanol. Therefore it is necessary to use the full formulation of equation (1), where the chemical potentials are expressed in terms of the species activities. For the activities an appropriate thermodynamic model is required, accounting for the special situation inside a swollen polymer. Such an activity model will be presented in the next section.

Moreover, the pressure-dependency of the chemical potentials (second term) can be neglected as here we have an incompressible (liquid) system at fairly low pressures. Also the third term of equation (1) (for viscous flow) can be skipped due to the very low permeability of the PEM (pore sizes in the nanometer range) and the necessarily limited pressure differences applied between anode and cathode [10] [11] .

The just mentioned simplifications lead to the following form of the Maxwell-Stefan equations for the mobile species ($j$ = H$^+$, H$_2$O, CH$_3$OH):

$$-c_j^M \frac{1}{a_j^M} \frac{\partial a_j^M}{\partial z} - z_j^* c_j^M \frac{F}{RT^M} \frac{\partial \phi^M}{\partial z} = \sum_{i \neq j} \frac{x_i^M n_j^M - x_j^M n_i^M}{\text{Ð}_{ij}^{M,eff}} + \frac{n_j^M}{\text{Ð}_{jM}^{M,eff}} \tag{2}$$

As the flux density of protons $n_{H^+}^M$ is given as fixed by the electric current density $i_{cell}$ using Faraday's law, only the flux densities of water and methanol have to be determined. They can be obtained explicitly from equation (1):

$$n_{CH_3OH}^M = \frac{L_{H_2O} + L_{CH_3OH} - n_{H^+} L_1 - n_{H_2O} L_2}{L_3} \tag{3}$$

with $\quad L_1 = -\dfrac{x_{H_2O}^M}{\text{Ð}_{H^+,H_2O}^{eff}} - \dfrac{x_{CH_3OH}^M}{\text{Ð}_{H^+,CH_3OH}^{eff}}$ , $L_2 = \dfrac{x_{H^+}^M}{\text{Ð}_{H^+,H_2O}^{eff}} + \dfrac{1}{\text{Ð}_{H_2O,M}^{eff}}$ , $L_3 = \dfrac{x_{H^+}^M}{\text{Ð}_{H^+,CH_3OH}^{eff}} + \dfrac{1}{\text{Ð}_{CH_3OH,M}^{eff}}$ ,

$$L_{H_2O} = -\frac{c_{H_2O}^M}{a_{H_2O}^M} \frac{\partial a_{H_2O}^M}{\partial z} \;,\; L_{CH_3OH} = -\frac{c_{CH_3OH}^M}{a_{CH_3OH}^M} \frac{\partial a_{CH_3OH}^M}{\partial z} \;,$$

$$n^M_{H_2O} = \frac{L_{H_2O} - n_{H^+}\left(L_4 - \dfrac{L_1 L_6}{L_3}\right) - (L_2 + L_3)\dfrac{L_6}{L_3}}{L_5 - \dfrac{L_2 L_6}{L_3}} \tag{4}$$

with $\quad L_4 = -\dfrac{x^M_{H_2O}}{\text{\DH}^{eff}_{H^+,H_2O}}$ , $L_5 = \dfrac{x^M_{H^+}}{\text{\DH}^{eff}_{H^+,H_2O}} + \dfrac{x^M_{CH_3OH}}{\text{\DH}^{eff}_{H_2O,CH_3OH}} + \dfrac{1}{\text{\DH}^{eff}_{H_2O,M}}$ , $L_6 = -\dfrac{x^M_{H_2O}}{\text{\DH}^{eff}_{H_2O,CH_3OH}}$ .

The electric potential gradient $\partial \phi^M / \partial z$ in the PEM material (transport resistance to the proton flux, i.e. Ohmic drop) is calculated from equation (1) for the protons as:

$$\frac{\partial \phi^M}{\partial z} = -\frac{R T^M}{c^M_{H^+} F}\left(L_{H^+} + n_{H^+} L_7 + n_{H_2O} L_8 + n_{CH_3OH} L_9\right) \tag{5}$$

with $\quad L_7 = \dfrac{x^M_{H_2O}}{\text{\DH}^{eff}_{H^+,H_2O}} + \dfrac{x^M_{CH_3OH}}{\text{\DH}^{eff}_{H^+,CH_3OH}} + \dfrac{1}{\text{\DH}^{eff}_{H^+,M}}$ , $L_8 = -\dfrac{x^M_{H^+}}{\text{\DH}^{eff}_{H^+,H_2O}}$ , $L_9 = -\dfrac{x^M_{H^+}}{\text{\DH}^{eff}_{H^+,CH_3OH}}$ ,

$$L_{H^+} = -\frac{c^M_{H^+}}{a^M_{H^+}}\frac{\partial a^M_{H^+}}{\partial z} \approx -\frac{c^M_{H^+}}{x^M_{H^+}}\frac{\partial x^M_{H^+}}{\partial z} \ .$$

The relative water content, i.e. the ratio between number of water molecules, $N^M_{H_2O}$ [mol], and number of sulfonic acid groups -$SO_3^-$, $N^M_{R-SO_3^-}$ [mol],

$$\Lambda^M = \frac{N^M_{H_2O}}{N^M_{R-SO_3^-}} \ , \tag{6}$$

can have values between 0 (totally dry membrane) and up to 30 (fully swollen with water and methanol at room temperature). Depending on local water and methanol content, thicknesses and porosities can vary significantly. Therefore it is not suitable to formulate mass balances in molar concentrations, as these refer to a constant overall volume. It is more convenient to use a concentration quantity which refers to the constant cross-sectional area of the cell, $A^S$ [m²]. This molar density $\hat{N}^M_j$ [mol m$^{-2}$] is defined as:

$$\hat{N}^M_j = \frac{N^M_j}{A^S} \ . \tag{7}$$

With this, in a spatially discretised model, mass balances for the PEM control volumes (index $k$) are given by:

$$\frac{d\hat{N}^M_{j,k}}{dt} = n^M_{j,k-1} - n^M_{j,k} \quad \text{with } j = H_2O, CH_3OH. \tag{8}$$

Swelling of the membrane is assumed to be in steady state. A total mass balance is not formulated, as pressures are not discussed within the membrane.

## PEM activity model

In the PEM material, the Flory-Huggins activity model for polmer-solvent mixtures [7] is applied. The activity of a species $j$ is given as a function of the volume fractions $\varepsilon_j$ [-] of all mobile species and the polymer backbone, treating the polymer backbone and the mobile species as a mixture :

$$a_j = \varepsilon_j \exp\left\{ \sum_{i \neq j}\left[\left(1 - \frac{\overline{V}_j}{\overline{V}_i}\right)\varepsilon_i + \chi_{j,i}\,\varepsilon_i^2\right] + \frac{\overline{V}_j}{2 \cdot N_{M,cu} \cdot \overline{V}_{M,cu}}\,\varepsilon_M^{1/3}\right\} \quad . \tag{9}$$

For the polymer material the species index "M" is used. For each pair of species, a non-ideality parameter $\chi_{j,i}$ [-] is required. Crosslinking of the polymer material is accounted for in the last term on the right hand side. $N_{M,cu}$ [-] is the number of sequential single polymer chain units (i.e. monomer units) within the main polymer chain between two cross-links (approx. 5 for NAFION™), $\overline{V}_{M,cu}$ [m³ mol⁻¹] is the molar volume of such a single chain unit. As the molar volume of the polymer is some orders of magnitude higher than those of the mobile species, the term $\left(1 - \overline{V}_j / \overline{V}_i\right)$ is approximately 1. In the following, three species are accounted for: The polymer backbone, water and methanol. From swelling experiments, the values of the non-ideality parameters were determined as:

$$\chi_{H_2O,M} = 0.72 \quad , \quad \chi_{CH_3OH,M} = 0.13 \quad , \quad \chi_{H_2O,CH_3OH} = 1.30 \quad .$$

## Energy and charge transport within the PEM

Energy transport in a porous structure can take place due to transport bound to the moving species and due to thermal conduction. The latter takes place in the mobile phase as well as in the stationary solid matrix. Additionally, within the membrane (M) spatially distributed heat production occurs (Joule heating), due to the transport of charged species in an electric field within a conducting phase with an Ohmic resistance. To account for these phenomena, two energy flux densities are introduced: Enthalpy flux densities $e^M$ [J m⁻² s⁻¹]

$$e^M = \sum_j e_j^M = \sum_j n_j^M\, h_j(T) \quad , \tag{10}$$

which are coupled to the flux densities $n_j^M$ [mol m⁻² s⁻¹] of the mobile species and their specific enthalpies $h_j$ [J mol⁻¹], and a heat flux density $q^M$ [J m⁻² s⁻¹] due to thermal conduction (Fourier´s law)

$$q^M = -\lambda^{M,eff}\,\frac{\partial T^M}{\partial z} \quad . \tag{11}$$

In equation (11) $\lambda^{M,eff}$ [W m⁻¹ K⁻¹] stands for the local effective thermal conductivity coefficient. The upper index "*eff*" denotes that it is dealt with a mixture of a fluid and a solid phase, which both contribute to thermal conduction. The effective thermal conductivity of wet NAFION™ is given as $\lambda^{M,eff} = 0.43\ \mathrm{W\,m^{-1}\,K^{-1}}$ in the literature [9] . Changes due to variation of local water and methanol contents are neglected. Finally, Joule heating $e_{Joule}^M$ [W m⁻³] due to the Ohmic resistance is given by

$$e_{Joule}^M = i\,\frac{\partial \phi^M}{\partial z} \quad . \tag{12}$$

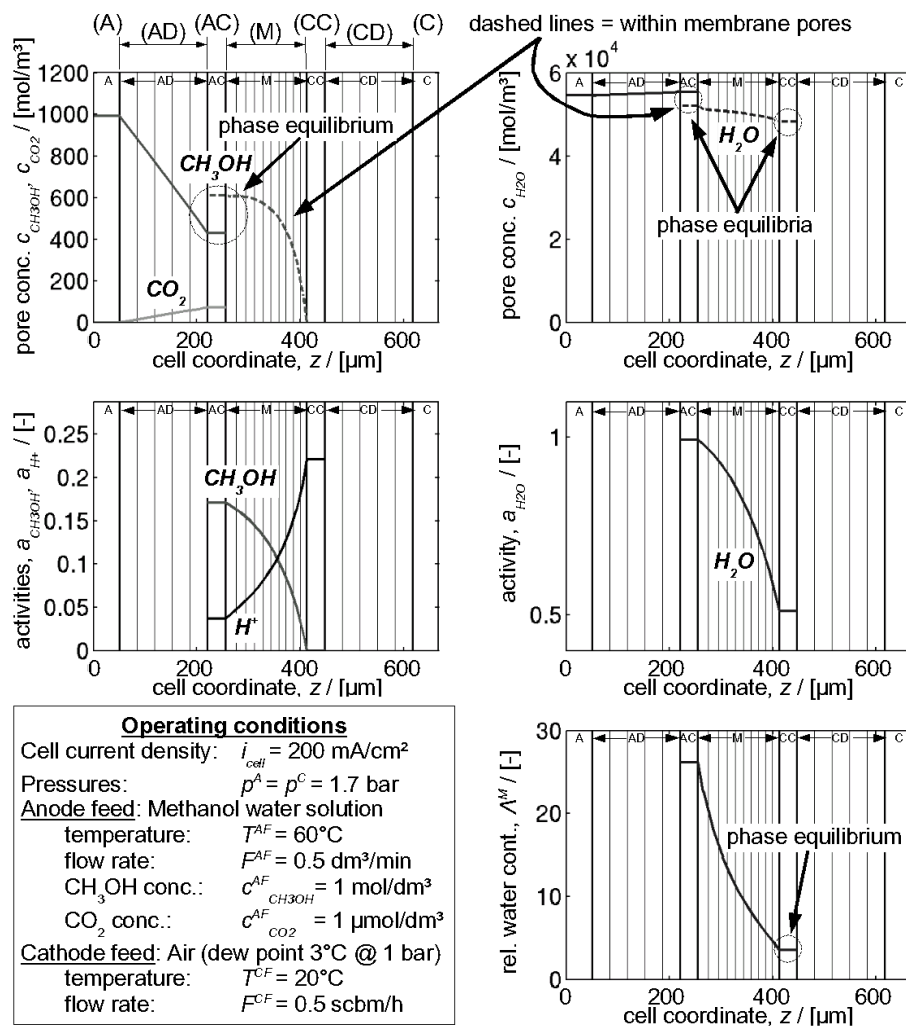Combining all three presented energy contributions yields the following one-dimensional energy balance of the PEM:

$$\frac{\partial T^M}{\partial t} = \frac{1}{(\rho C_p)^M}\left[-\frac{\partial e^M}{\partial z} - \frac{\partial q^M}{\partial z} + e^M_{Joule}\right] \quad . \tag{13}$$

Charge transport in the PEM is bound to protons. Therefore, the charge flux density $i^M$ [A m$^{-2}$] equals the electric cell current density, and the proton flux is given by Faraday`s law . As in the PEM neither charge production nor accumulation occurs, one obtains the quasi-stationary charge balance:

$$0 = -\frac{\partial i^M}{\partial z} \quad . \tag{14}$$

## Simulation results

As the model is one-dimensional perpendicular to the cell plane, profiles through the DMFC are obtained for concentrations, temperature, pressure and all presented fluxes. Selected steady-state profiles are shown in Figure 2 . The abscissae show the real cell geometry with respect to the thicknesses of the different layers of the DMFC. The vertical lines represent the limits of the control volumes, illustrating the spatial discretisation of both diffusion layers (AD,CD) and the PEM (M). As introduced, the thicknesses of the diffusion layer control volumes are constant (solid matrix) while those of the membrane control volumes change due to swelling.

The most interesting concentration profiles develop within the membrane (dashed concentration profiles in the upper two diagrams of Figure 2). The methanol pore concentration shows a strongly bent profile in the direction of the overall flow, i.e. towards the cathode. This makes sense as methanol is dragged along with the water flow (diffusion and electro-osmosis). Also the water profile is slightly bent in the same



### Operating conditions

| Cell current density: | $i_{cell}$ = 200 mA/cm² |
|---|---|
| Pressures: | $p^A = p^C$ = 1.7 bar |

Anode feed: Methanol water solution
  temperature: $T^{AF}$ = 60°C
  flow rate: $F^{AF}$ = 0.5 dm³/min
  CH$_3$OH conc.: $c^{AF}_{CH3OH}$ = 1 mol/dm³
  CO$_2$ conc.: $c^{AF}_{CO2}$ = 1 µmol/dm³
Cathode feed: Air (dew point 3°C @ 1 bar)
  temperature: $T^{CF}$ = 20°C
  flow rate: $F^{CF}$ = 0.5 scbm/h

**Figure 2** Simulated steady state profiles

manner due to electro-osmotic transport. Nonetheless, diffusion remains the major mode of transport for methanol and water. Most interesting is the big difference in the water content between anode and cathode side of the membrane. While on the anode side a relative water content of around 26 is reached, on the cathode side only values around 4 are found. This is due to the operation of the cell with dry air (dew point 3°C) at high cathode flow rates. Water is transported away from the cathode catalyst layer (CC) very efficiently, drying out this side of the membrane. This change in water content is also illustrated by the decreasing thickness of the membrane control volumes from anode to cathode.

With the model, series of simulations were conducted, to compare those data with experimental results. Figure 3 shows selected steady state simulation results and corresponding experimental data. It has to be emphasised that all simulation results are obtained using the same set of parameters taken from the literature. As one can see from Figure 3, in general a reasonable approximation to the experimental steady state results was achieved. The simulation results are in the orders of the experimental membrane crossover flux densities and the current-voltage curves, and also the trends are predicted correctly, i.e. water crossover fluxes increase with current density and methanol crossover fluxes decrease with current density.

## Conclusions

The presented DMFC model yields good approximations to experimental data with respect to mass transport (crossover) for a variety of fuel cell operating conditions using only one single set of parameters.

From the simulation results, it is possible to evaluate the importance of the different mass transport contributions (driving forces and friction) in the generalised Maxwell-Stefan framework, equation (1). Table 1 presents the quintessence of this evaluation. In the top line, the complete equation (1) is given. In the following rows the importance of the individual
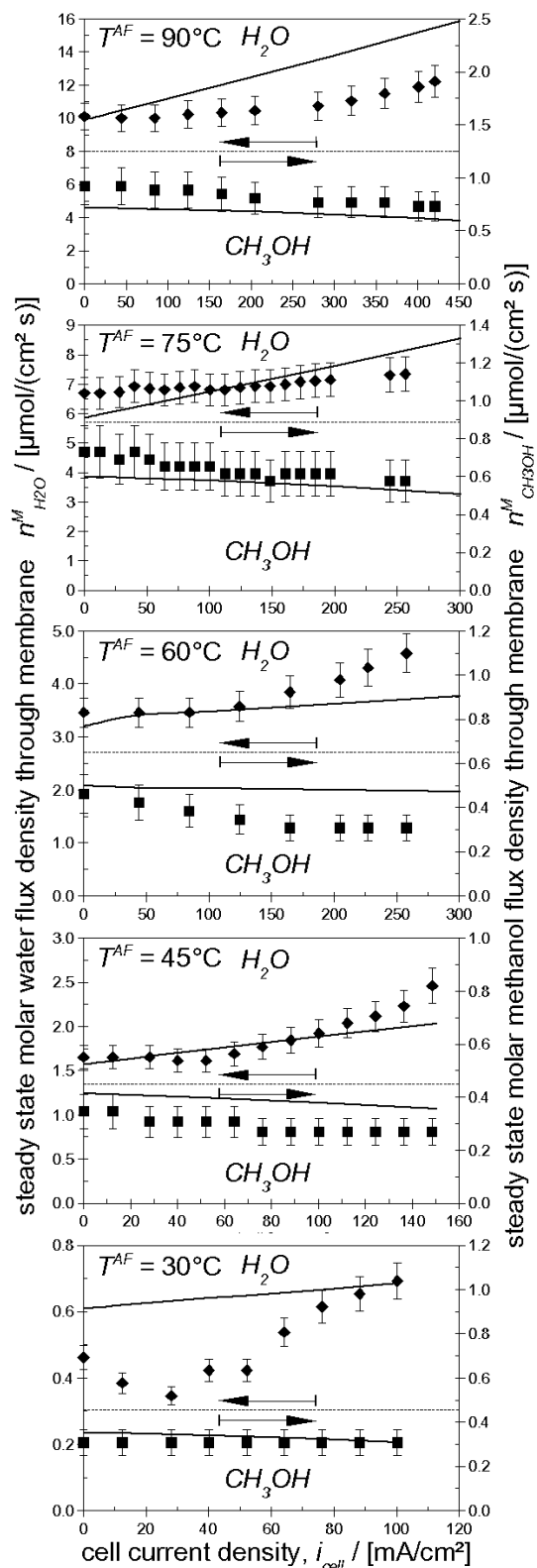


**Figure 3** Experimental (symbols) and simulated (lines) crossover flux densities (left y-axis: water, right y-axis: methanol); Operating conditions as in Figure 2, anode feed temperature varied

terms is indicated for each mobile species by "++" (very important), "+" (moderately important) and blanks (not important/negligible):

**Table 1** Importance of mass transport contributions in equation (1)
(driving forces and friction terms):
++ = very important, + = important, blanks = not important/negligible

$$ -\frac{c_j}{RT}\nabla_{T,p}\,\mu_j \;-\; \frac{c_j}{RT}\overline{V}_j\,\nabla p \;-\; \frac{\alpha_j{}'}{Đ_{jM}}c_j\frac{B_0}{\eta}\nabla p \;-\; c_j z_j^{*}\frac{F}{RT}\nabla\phi \;=\; \sum_{i\neq j}\frac{x_i n_j - x_j n_i}{Đ_{ij}^{eff}} \;+\; \frac{n_j}{Đ_{jM}^{eff}} $$

| | | $-\frac{c_j}{RT}\nabla_{T,p}\mu_j$ | $-\frac{c_j}{RT}\overline{V}_j\nabla p$ | $-\frac{\alpha_j'}{Đ_{jM}}c_j\frac{B_0}{\eta}\nabla p$ | $-c_j z_j^*\frac{F}{RT}\nabla\phi$ | $\sum_{i\neq j}\frac{x_i n_j - x_j n_i}{Đ_{ij}^{eff}}$ | $\frac{n_j}{Đ_{jM}^{eff}}$ |
|---|---|---|---|---|---|---|---|
| | H$^+$ | ++ | | | ++ | ++ | ++ |
| (M) | H$_2$O | ++ | | | | ++ | ++ |
| | CH$_3$OH | ++ | | | | ++ | + |

Obviously, multi-component diffusion represented by the gradient in the chemical potentials as driving force, left term, and both friction terms (species-species and species-matrix), right side of equation (1), are the most important influencing factors for mass transport of all mobile species within the PEM. The pressure-dependence of the chemical potentials (second driving force term on the left hand side of equation (1)) is negligible, which is generally justified for liquid phases if no large pressure gradients exist. This term is only relevant for applications with extremely high pressure differences as they can be found e.g. in reverse osmosis and pervaporation processes. The third driving force is pressure-driven convection. Within the PEM this term is negligible due to the low hydraulic permeability (pore diameters in the nanometer range). Finally, the electric field as driving force only plays a role for protons, which are the only mobile species carrying a charge.

Obviously, in the DMFC electro-osmotic flow only plays a minor role compared to diffusive transport of water and methanol across the PEM. Therefore the situation is much different from that in a typical PEMFC operated on hydrogen and air.

**References**

[1]  L. Carrette, K.A. Friedrich and U. Stimming, *Fuel Cells 1 No. 1* (2001) 5.
[2]  T. Schultz, S. Zhou and K. Sundmacher, *Chem. Eng. Technol. 24 No.12* (2001) 1223.
[3]  T. Schultz, *Experimental and Model-based Analysis of the Steady-state and Dynamic Operating Behaviour of the Direct Methanol Fuel Cell (DMFC)*, Dissertation thesis, Otto-von-Guericke University Magdeburg, 2004.
[4]  K. Sundmacher and K. Scott, *Chem. Eng. Sci. 54* (1999) 2927.
[5]  S. Zhou, T. Schultz, M. Peglow and K. Sundmacher, *Phys. Chem. Chem. Phys. 3 No. 3* (2001) 347.
[6]  A. Siebke, W. Schnurnberger, F. Meier and G. Eigenberger, *Fuel Cells 3 No.1* (2003) 1.
[7]  J. A. Wesselingh and R. Krishna, *Mass Transfer in Multicomponent Mixtures,* Delft University Press, Delft, 2000
[8]  R. Krishna and J. A. Wesselingh, *Chem. Eng. Sci. 52 No. 6* (1997) 861.
[9]  M. Wöhr, K. Bolwin, W. Schnurnberger, M. Fischer, W. Neubrand and G. Eigenberger, *Int. J. Hydrogen Energy 23 No. 3* (1997) 213.
[10] F. Meier, F. Denz, A. Weller and G. Eigenberger, *Fuel Cells 3 No. 4* (2004) 161.
[11] G. J. M. Janssen and M. L. J. Overvelde, *J. Power Sources 101 No.1* (2001) 117.